

## ITC analysis of polydisperse systems

Unravelling the impact of sample heterogeneity

Schönbeck, Christian; Kari, Jeppe; Westh, Peter

*Published in:*  
Analytical Biochemistry

*DOI:*  
[10.1016/j.ab.2023.115446](https://doi.org/10.1016/j.ab.2023.115446)

*Publication date:*  
2024

*Document Version*  
Publisher's PDF, also known as Version of record

*Citation for published version (APA):*  
Schönbeck, C., Kari, J., & Westh, P. (2024). ITC analysis of polydisperse systems: Unravelling the impact of sample heterogeneity. *Analytical Biochemistry*, 687, Article 115446. <https://doi.org/10.1016/j.ab.2023.115446>

### General rights

Copyright and moral rights for the publications made accessible in the public portal are retained by the authors and/or other copyright owners and it is a condition of accessing publications that users recognise and abide by the legal requirements associated with these rights.

- Users may download and print one copy of any publication from the public portal for the purpose of private study or research.
- You may not further distribute the material or use it for any profit-making activity or commercial gain.
- You may freely distribute the URL identifying the publication in the public portal.

### Take down policy

If you believe that this document breaches copyright please contact [rucforsk@kb.dk](mailto:rucforsk@kb.dk) providing details, and we will remove access to the work immediately and investigate your claim.



# ITC analysis of polydisperse systems: Unravelling the impact of sample heterogeneity

Christian Schönbeck<sup>a,\*</sup>, Jeppe Kari<sup>b</sup>, Peter Westh<sup>c</sup>

<sup>a</sup> Department of Pharmacy, University of Copenhagen, Denmark

<sup>b</sup> Department of Science and Environment, Roskilde University, Denmark

<sup>c</sup> Department of Biotechnology and Biomedicine, Technical University of Denmark, Denmark

## ABSTRACT

Binding interactions often involve heterogeneous samples displaying a distribution of binding sites that vary in affinity and binding enthalpy. Examples include biological samples like proteins and chemically produced samples like modified cyclodextrins. Experimental studies often ignore sample heterogeneity and treat the system as an interaction of two homogeneous species, i.e. a chemically well-defined ligand binding to one type of site. The present study explores, by simulations and experiments, the impact of heterogeneity in isothermal titration calorimetry (ITC) setups where one of the binding components is heterogeneous. It is found that the standard single-site model, based on the assumption of two homogeneous binding components, provides excellent fits to simulated ITC data when the binding free energy is normally distributed and all sites have similar binding enthalpies. In such cases, heterogeneity can easily go undetected but leads to underestimated binding constants. Heterogeneity in the binding enthalpy is a bigger problem and may result in enthalpograms of increased complexity that are likely to be misinterpreted as two-site binding or other complex binding models. Finally, it is shown that heterogeneity can account for previously observed experimental anomalies. All simulations are accessible in Google Colab for readers to experiment with the simulation parameters.

## 1. Introduction

Ligand-binding plays an integral role in a myriad of industrial applications and research fields, and many experimental techniques have been developed for the precise determination of binding affinities. However, most analyses of experimental data do not take into account the intricacies introduced by samples containing multiple, non-identical ligands or receptors, each with unique affinities. Modelling the interaction as if it involves two monodisperse binding partners is a potential source of error on the determined binding affinity.

Isothermal titration calorimetry (ITC) is an often-used method for measuring binding affinities of bio-molecular systems, such as protein-ligand binding. The method relies on the heat of binding, and ITC is thus capable of measuring binding affinities in all systems that produces a heat signal, provided that the binding affinity is within a suitable range. The binding affinity, expressed as the binding constant, dissociation constant, or free energy of binding, is obtained by fitting a suitable binding model to the heat signals from the titration experiment. Most works employ a binding model, the single-site model (often called “one set of sites” model in the literature), which assumes the presence of a number ( $N$ ) of identical and independent binding sites (Scheme 1).

This model assumes each of the binding partners to be

homogeneous/monodisperse, i.e. each binding partner should consist of only one well-defined chemical species. However, this may not always be the case. A protein, for example, may undergo post-translational modifications to produce a heterogeneous sample containing a broad distribution of differently modified proteins. A sample of glycoprotein with a well-defined amino acid sequence may consist of numerous glycoforms differing in the extent and pattern of glycosylation as well as the type of attached glycans [1]. The ligand may have a different affinity for each of these protein species, and the single-site model thus seems inadequate. In general, biological samples and their derivatives often consist of a multitude of structurally distinct species, and it is often a near-impossible task to purify single species in the amounts required for ITC binding experiments. Thus, ITC binding experiments are often performed with heterogeneous samples. Examples of ITC studies with heterogeneous samples include the binding of drug molecules to glycoproteins [2] and glucosaminoglycans [3], metal ions binding to mixtures of lignin degradation products [4], binding of a fluorescent dye to a thermally stressed antibody [5], and the formation of host-guest complexes with modified cyclodextrins [6].

The single-site model cannot be expected to be an adequate description of heterogeneous systems but is nevertheless often applied to ITC experiments in which one of the components is heterogeneous; with

\* Corresponding author.

E-mail address: [christian.schonbeck@sund.ku.dk](mailto:christian.schonbeck@sund.ku.dk) (C. Schönbeck).



**Scheme 1.** Definition of the equilibrium constant,  $K$ , for the binding of  $H$  to  $M$ .  $H$  is a molecule,  $M$  is a binding site on a molecule containing  $N$  identical and independent binding sites, and  $C$  is the complex consisting of  $H$  bound to  $M$ . This scheme is referred to as the single-site model (or “one set of sites model”) as all binding events are characterized by the same equilibrium constant and binding enthalpy.

apparent success as judged from the good fit of the model to experimental data [6,7]. In fact, binding experiments with heterogeneous samples of modified cyclodextrins are routinely fitted with the single-site model to yield the binding constant, binding enthalpy and binding stoichiometry as fitting parameters [8,9]. An important question emerges: if the single-site model is too simplistic, can the obtained fitting parameters be trusted? Is the single-site model capable of fitting the data, and does sample heterogeneity bias the results?

To answer these questions, ITC data are simulated for a system consisting of a homogeneous (Monodisperse) component,  $M$ , binding to a Heterogeneous component,  $H$ . The simulated system thus consists of multiple linked binding equilibria, each representing the  $M$  component binding to one of the multiple  $H$  fractions of the heterogeneous component  $H$ . The single-site model is then fitted to the simulated data to explore the impact on the apparent binding parameters. It is further shown that sample heterogeneity can account for previously observed experimental anomalies.

The present work is inspired by previous ITC studies of the binding of homogeneous samples of small guest molecules to heterogeneous samples of cyclodextrin host molecules and draws on some of the experimental data from these works [6,10,11]. Cyclodextrin host-guest complexes possess ideal properties for the study by ITC and are therefore suitable model systems for the study of more general binding phenomena. The heterogeneity of the cyclodextrin samples is due to the random attachment of substituents (for example hydroxypropyl) to a number of sites on the cyclodextrins, resulting in samples containing a distribution of modified cyclodextrin molecules that differ in the degree and pattern of substitution (Fig. S1) [10].

## 2. Theoretical background and methods

### 2.1. The ITC experiment

In a standard ITC experiment one binding partner is titrated into the other and the resulting heat of binding is monitored as the titration progresses. Plotting the measured heats,  $q$ , as a function of the molar ratio produces an enthalpogram (Fig. 1) which is typically fitted with the single-site model to yield the binding constant,  $K$ , the binding enthalpy,  $\Delta H$ , and the number of identical and independent binding sites on the component in the titration cell,  $N$ . The binding constant is often converted to the standard Gibbs free energy of binding by the use of equation (1).

$$\Delta G^\circ = -RT \ln(K) \quad (1)$$

Concentrations of the components in the titration cell and syringe are typically chosen such that the injected moles of syringe component at the end of the titration is around twice the moles of cell component. Further, to obtain suitably shaped enthalpograms for accurate determination of binding parameters the so-called Wiseman  $c$ -value,  $c = M_t K$  ( $M_t$  being the total concentration of the component in the cell), should be in the range 1–1000 [12], and preferably 5–500 [13].

### 2.2. Distribution of heterogeneous component, $H$

In the following, it is assumed that the heterogeneous component,  $H$ , is comprised of species that are normally distributed with respect to  $\ln$

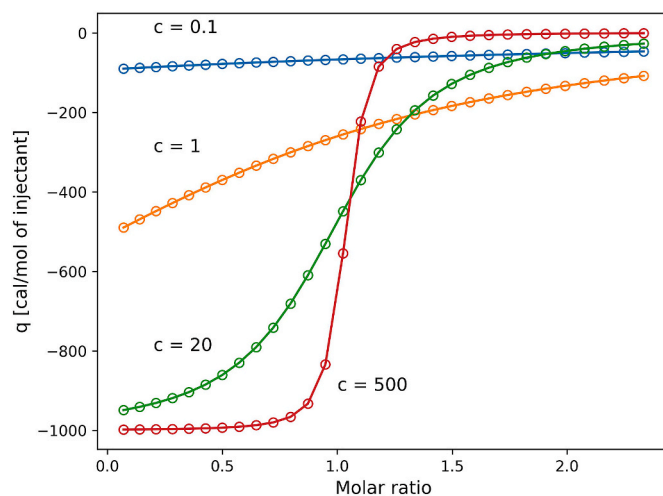


**Fig. 1.** Simulated ITC enthalpograms for the binding of two homogeneous components according to the single-site model. The higher the Wiseman  $c$ -value, the steeper the curve at the inflection point. No inflection point occurs at low values of  $c$ . Parameters  $N$  and  $\Delta H$  are 1.0 and  $-1000$  cal/mol.

( $K$ ), equivalent to a normal distribution in  $\Delta G^\circ$ . The species of  $H$  then follow a lognormal distribution with respect to  $K$  (Fig. 2), as previously reported [14]. The distributions are defined by a mean,  $\mu$ , and a standard deviation,  $\sigma$ .

From the properties of lognormal distributions [15] and equation (1), the mean and standard deviation of  $K$  can be converted into a mean and standard deviation of  $\Delta G^\circ$ :

$$\sigma_{\Delta G} = RT \sqrt{\ln \left( 1 + \left( \frac{\sigma_K}{\mu_K} \right)^2 \right)} \quad (2)$$

$$\mu_{\Delta G} = -RT \left[ \ln(\mu_K) - 0.5 \left( \frac{\sigma_{\Delta G}}{RT} \right)^2 \right] \quad (3)$$

### 2.3. Heterogeneity in $\Delta H$

Each species of  $H$  may not only possess a different binding affinity towards  $M$  but may also differ in the heat of binding, which is the observable in ITC. Heterogeneity in the heat of binding,  $\Delta H$ , will thereby affect the obtained enthalpograms and fitting parameters. For cyclodextrin homologues, both  $\Delta G^\circ$  and  $\Delta H$  seems linearly related to the degree of structural modifications [10], and a linear relationship between  $\Delta G^\circ$  and  $\Delta H$  is therefore assumed. Thus, if the species of  $H$  are normally distributed with respect to  $\Delta G^\circ$  they are also normally distributed with respect to  $\Delta H$ . However, the width of the distributions need not be the same. In fact, it is often observed that  $\Delta H$  spans a much larger range than  $\Delta G^\circ$  – a phenomenon termed enthalpy-entropy compensation.

### 2.4. Simulation of enthalpograms for heterogeneous systems

In contrast to most methods for determination of binding constants the experimental observable in ITC is not proportional to the number of formed complexes. Instead, the produced heat is proportional to the *increment* in the number of complexes for each injection in the titration. Simulation of an ITC enthalpogram involves calculation of 1) the number of formed complexes at each step of the titration 2) the total amount of produced heat and 3) the incremental heat,  $q$ .

The concentrations of formed complexes,  $[C_i]$ , were found by numerically solving the system of equations comprised by the law of mass action for the  $n$  linked binding equilibria:

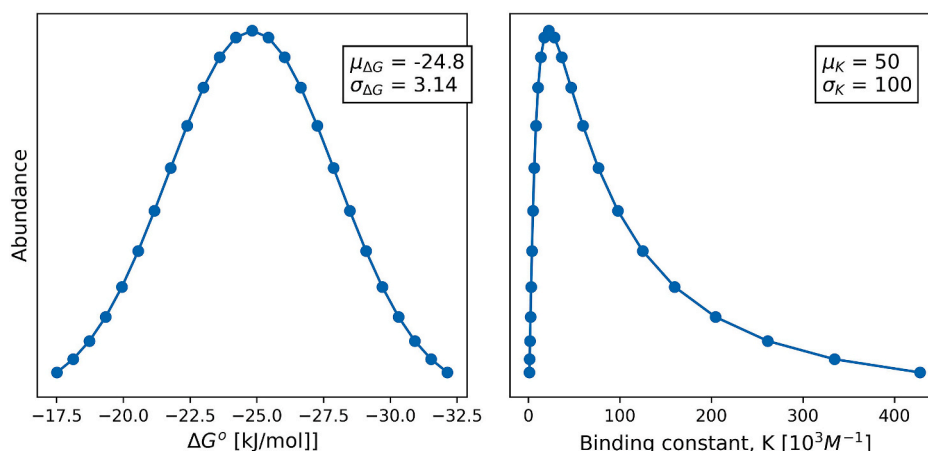


**Fig. 2.** 25 species (circles) of heterogeneous component **H** normally distributed with respect to  $\Delta G^\circ$  (in kJ/mol) and the corresponding lognormal distribution of **K** (in units of  $10^3 M^{-1}$ ). The distributions are truncated in both ends to contain 98 % of the infinite distribution.

$$K_i = \frac{[C_i]}{[H_i][M]} \quad (4)$$

and the mass balances of **H** and **M**:

$$M_t = [M] + \sum_{i=1}^n [C_i] \quad (5)$$

$$H_{t,i} = [H_i] + [C_i] \quad (6)$$

For known total concentrations of the homogeneous component,  $M_t$ , and each of the heterogeneous species  $H_{t,i}$ , these  $2n+1$  equations with  $2n+1$  unknowns ( $n[H_{t,i}]$ ,  $n[C_i]$  and  $[M]$ ) were numerically solved to yield the concentrations of complexes.

The total produced heat,  $Q$ , was then calculated by multiplying the produced moles of complexes with their respective binding enthalpies:

$$Q = V_0 \sum_{i=1}^n [C_i] \Delta H_i \quad (7)$$

where  $V_0$  is the volume of the calorimetric cell.

Finally, the incremental heats,  $q$ , were calculated and plotted as a function of the ratio of the concentrations of titrator to titrand in the calorimetric cell. The reader is referred to the ITC user manual [16] for the exact procedure for calculation of titrator and titrand concentrations and the incremental heat. No artificial noise was added to the simulated data.

Simulations resembled a typical experimental setup on a VP-ITC instrument with a 1.436 ml calorimetric cell. Titrations consisted of thirty 10  $\mu$ L aliquots of 10 mM titrator solution into 1 mM titrand solution. The parameter  $N$  was treated as a correction factor to the titrand concentration, as is usually done in ITC analysis. All simulations were carried out with the same mean value of the binding enthalpy,  $\mu_{\Delta H} = -1000$  cal/mol.

Simulations and fits to experimental data were conducted in Python. All code is made publicly available in Google Colab as executable code that generates the exact figures and results that are presented in this manuscript. Readers are encouraged to visit the Colab notebook and experiment with the simulation parameters: <https://colab.research.google.com/drive/1vceKln9h9vSUSTX9e3HxQfxF9OU-WWc3?usp=sharing>.

### 3. Results

The following explores the impact of binding heterogeneity in systems of moderate binding affinities,  $K = 1-1000 \times 10^3 M^{-1}$ . The conclusions, however, are directly transferable to systems of higher or lower

affinities as it is not the binding affinity in itself but the Wiseman  $c$ -value that is the important parameter. The simulations were conducted with a cell concentration of 1 mM. An average binding constant of  $100 \times 10^3 M^{-1}$  then yields a Wiseman  $c$ -value of 100. Identical results would be obtained for other systems with the same Wiseman  $c$ -value, f.ex. a cell concentration of 1  $\mu$ M and an average binding constant of  $100 \times 10^6 M^{-1}$  (assuming that the standard deviation of  $K$  is scaled with the same factor).

#### 3.1. Heterogeneity in $K$ , constant $\Delta H$

A simulated enthalpogram for the titration of **M** with **H** is shown in Fig. 3A along with the fitting parameters obtained from fitting the single-site model to the simulated data.  $\mu_K$  and  $\sigma_K$  were set to  $50 \times 10^3 M^{-1}$  and  $100 \times 10^3 M^{-1}$ , respectively. Despite the broad distribution of  $K$  the single-site model gives an almost perfect fit, although with some systematic variation in the residuals. In a real-life situation such a fit would be considered absolutely satisfactory and would not lead to any suspicion that the single-site model is too simplistic. The simulated data do not reveal the actual complexity of the system. The fitting parameters are not a cause of suspicion either. The stoichiometry parameter,  $N$ , is close to unity, suggesting one-to-one binding, and the apparent binding enthalpy is quite close to the set value of  $-1000$  cal/mol. The apparent binding constant, however, is more than 3 times smaller than  $\mu_K$ .

Fig. 3b shows the gradual saturation of **M** by the injected species. Initially, there is plenty of free **M** in the cell, and most of the injected **H** species bind to **M**. This is reflected in the initial slopes of the lines which are close to 1. Only the weakest binders do not bind to a significant extent. As the equimolar ratio is approached the injected **H**'s start competing for the still fewer unbound **M**, and the strong binders start stealing **M** from the weak binders. That is, the weak complexes actually start dissociating, as reflected in the decreasing saturation curves. Despite the obvious differences in the saturation of **M** by the various **H**'s the total saturation of **M** resembles a normal binding isotherm for homogeneous binding. The differences in the individual binding isotherms seem to average out to produce a regular single-site isotherm. However, **M** is saturated a little slower than what is predicted by the single-site model with  $K$  set to  $\mu_K$ .

Simulation of the reverse titration with **H** in the cell and **M** in the syringe results in a very similar enthalpogram (Fig. 3C) and similar fit parameters. The saturation plot in Fig. 3D, however, reveals striking differences in the saturation pattern. When **H** was in the syringe, all injected species bound to **M** in the initial part of the titration, and competition for **M** did not set in until the equivalence point was approached. With **H** in the cell the situation is very different. The initial small amounts of injected **M** results in strong competition among the **H**'s

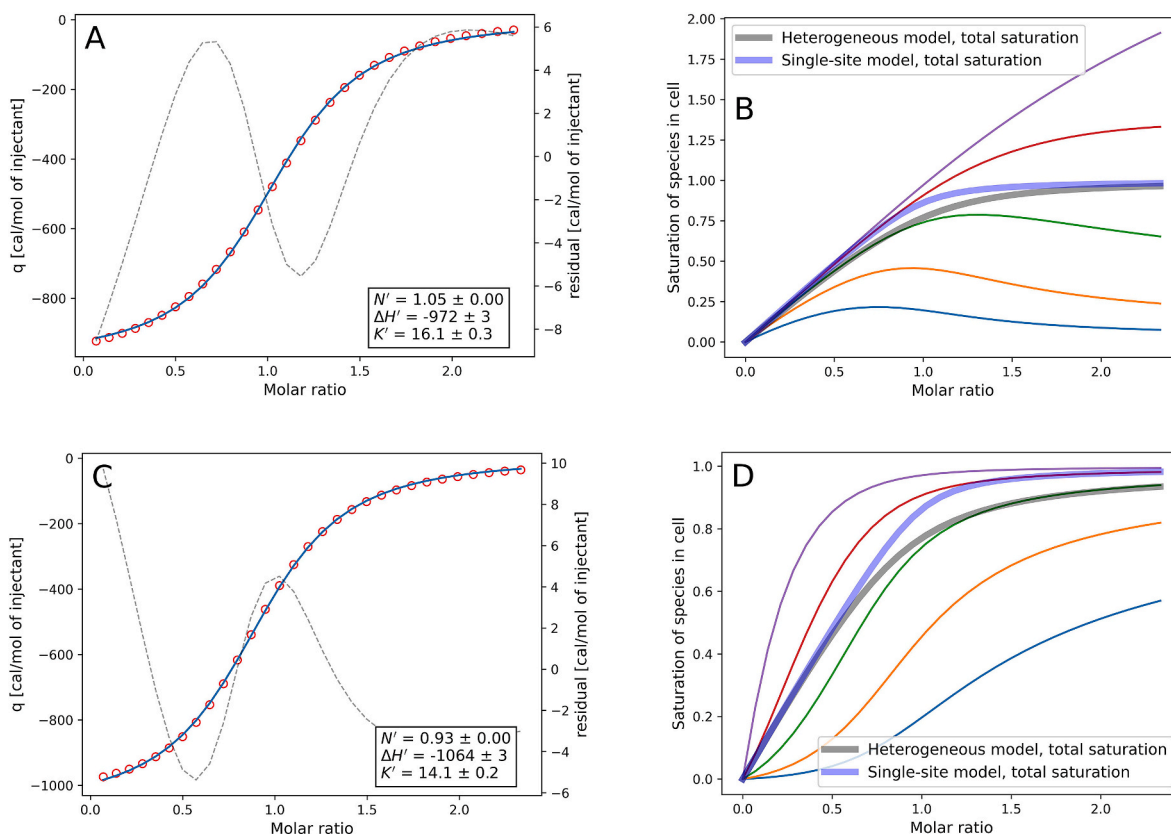


**Fig. 3.** Simulated enthalpograms and saturation curves for the titration of 10 mM **H** into 1 mM **M** (A and B) and titration of 10 mM **M** into 1 mM **H** (C and D). Simulated reaction heats (circles) are plotted together with the fit of the single-site model (solid line), residuals from the fit (broken line, right axis) and the resulting fit parameters (box).  $K$  and  $\Delta H$  are in units of  $10^3 \text{ M}^{-1}$  and cal/mol. Simulation parameters were:  $\mu_K = 50 \times 10^3 \text{ M}^{-1}$ ,  $\sigma_K = 100 \times 10^3 \text{ M}^{-1}$ ,  $N = 1.0$ ,  $\Delta H = -1000 \text{ cal/mol}$ . **H** contains 25 species but individual saturation curves are only shown for 5 representative species. The individual saturation curves in B represent the saturation of **M** by various  $H_i$ . To represent these on the same scale, each curve was divided by the fraction of  $H_i$ , resulting in values exceeding 1.

in the cell for binding to **M**. First the strong binders are saturated and then the weak binders. Competition for **M** gradually decreases throughout the titration as more **M** is injected.

### 3.2. Heterogeneity-induced “errors” on $K$ and $\Delta G^\circ$

The above simulations with  $\mu_K = 50 \times 10^3 \text{ M}^{-1}$  and  $\sigma_K = 100 \times 10^3 \text{ M}^{-1}$  produced enthalpograms that hardly deviated from normal single-site binding. Thus, heterogeneity was hardly detectable but nevertheless resulted in an apparent binding constant,  $K'$ , which was around 3–4 times lower than  $\mu_K$ . The two other fit parameters,  $\Delta H$  and  $N$ , were close to their real values. Is this result only valid for the specific choice of distribution parameters? This question was examined by generating distributions for many sets of relevant values of  $\mu_K$  and  $\sigma_K$  and fitting the single-site model to the simulated enthalpograms. The results for the titration of **H** into **M** are shown in Fig. 4.

Fig. 4A shows that heterogeneity always results in an apparent  $K$  that is lower than the average of the distribution. This is an intuitive result as the presence of many binding sites will cause a less defined saturation point, meaning a flattened enthalpogram and consequently a lower binding constant (see Fig. 1). This effect is more pronounced at high values of  $\mu_K$  than at low values where heterogeneity has a lower impact on the already “flat” enthalpograms.

In ITC, the obtained binding constant is often converted to a binding free energy,  $\Delta G^\circ$ , by means of equation (1), and the entropy of binding is subsequently found from  $\Delta G^\circ$  and  $\Delta H$ . The impact of heterogeneity on the apparent binding free energy,  $\Delta G' = -RT \ln(K')$ , was therefore examined by transforming Fig. 4A to the corresponding plot for  $\Delta G^\circ$  (Fig. 4B). Equations (2) and (3) transforms the x- and y-coordinates, and

the z-coordinate was transformed as:

$$\Delta G' - \mu_{\Delta G} = -RT \left[ \ln \left( \frac{K'}{\mu_K} \right) + 0.5 \left( \frac{\sigma_{\Delta G}}{RT} \right)^2 \right] \quad (8)$$

It is noteworthy that the difference between  $\Delta G'$  and  $\mu_{\Delta G}$  (equation (8)) depends not only on the “error” on the apparent  $K$  (the logarithmic term), but also on the width of the distribution ( $\sigma_{\Delta G}$ ). Fig. 4A shows that  $K'$  is always smaller than  $\mu_K$ , resulting in a negative value of the logarithmic term, but this is countered by the positive contribution of the last term. The peculiar consequence is that the apparent binding free energy differs relatively little from  $\mu_{\Delta G}$ , and may even be lower (more negative) than  $\mu_{\Delta G}$ , even though the apparent  $K$  is *always* smaller than  $\mu_K$ . Interestingly, the 0.0 contour line in Fig. 4B is almost horizontal. This means that for a sample with an average binding free energy of around 19 kJ/mol an ITC experiment of this heterogeneous system will yield an apparent binding free energy that is very close to the sample average, irrespective of the width of the distribution. In this case the ITC experiment yields the true sample average! It may seem odd that the apparent  $K$  deviates from the sample average while the apparent  $\Delta G^\circ$  does not. After all,  $K$  and  $\Delta G^\circ$  are just two different measures of the binding affinity. This perplexing fact is a consequence of the non-trivial relationship between the sample averages of  $K$  and  $\Delta G^\circ$ , expressed in equation (3) and deriving from the non-linear transformation between the distributions of  $K$  and  $\Delta G^\circ$ .

In general,  $\Delta G'$  deviates only little from the true sample average, except for broad distributions of the tight-binding samples (or more precisely, experiments with a high Wiseman  $c$ -value). For comparison, experimental errors in real-life determination of  $\Delta G^\circ$  are under the best circumstances around 0.25 kJ/mol, equivalent to a 10 % error in  $K$  [17].

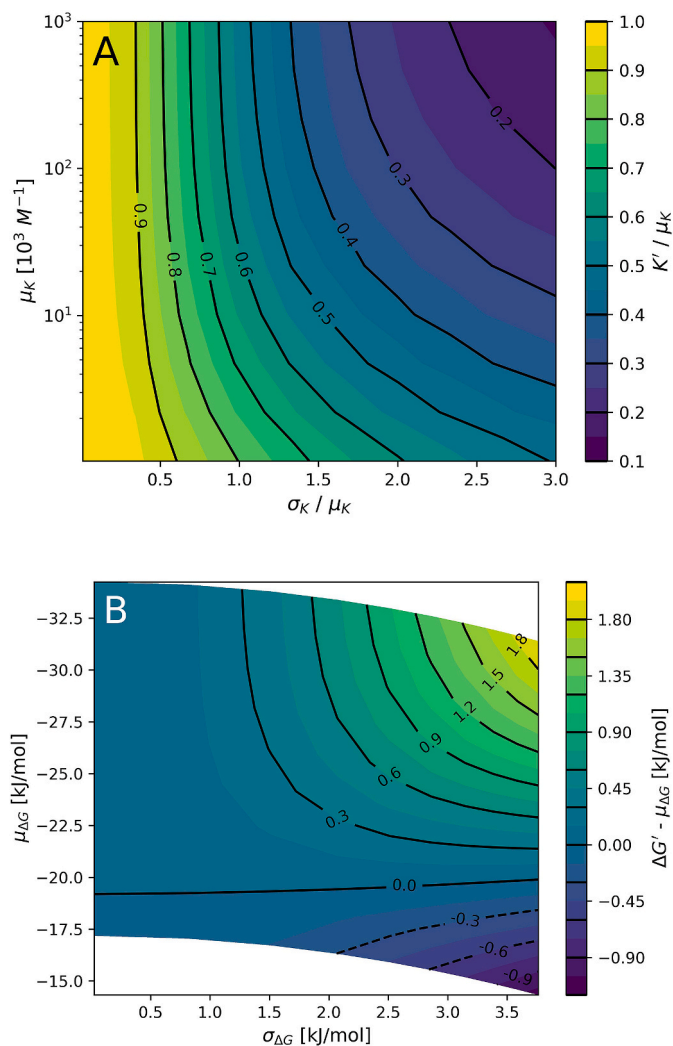


**Fig. 4.** Plots of the heterogeneity-induced deviation of A) the apparent binding constant,  $K'$ , and B) the apparent binding free energy,  $\Delta G'$ , from the real mean values of the distributions. Simulations are for titration of 10 mM **H** into 1 mM **M**. Figure B is a transformation of the data in A, and the downwards-bending grid and white spaces in B is a result of the y-coordinate ( $\mu_{\Delta G}$ ) depending on both the y-coordinate in A ( $\mu_{\kappa}$ ) and the x-coordinate in B ( $\sigma_{\Delta G}$ ) (see equation (3)).

The heterogeneity-induced “error” on the determined  $\Delta G^{\circ}$  is thus less or equivalent to the experimental error within large parts of the investigated range. Titrating **M** into **H** produces very similar results although  $K'$  and  $\Delta G'$  tend to deviate slightly more from the true sample means (Figs. S2 and S3).

### 3.3. Heterogeneity-induced errors on $N$ and $\Delta H$

The relative error on the remaining two fitting parameters,  $N'$  and  $\Delta H'$ , is much smaller than the relative errors on  $K$  (Fig. 5). For titrations of **H** into **M**,  $N'$  is slightly too large and only deviates significantly from its true value for broad distributions of weakly binding **H**, as observed in the lower right corner of Fig. 5.  $\Delta H'$  is inversely correlated to  $N'$  and its numerical value decreases when  $N'$  increases. These trends are a consequence of enthalpograms without inflection points (see Fig. 1). The ITC practitioner should always be wary of trusting the results from fits to such enthalpograms, and the significant deviation of  $N'$  from the expected value should lead to skepticism. It is therefore unlikely that the erroneous fitting parameters in the lower right corners of Fig. 5 will be trusted. Similar results, albeit with slightly larger errors, are obtained for

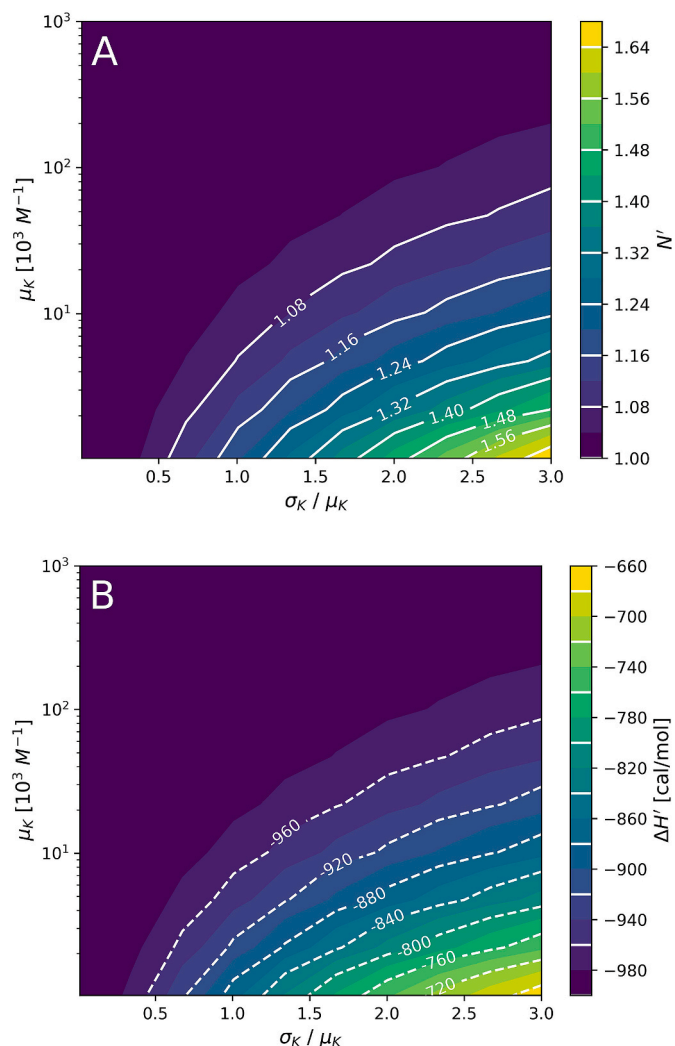


**Fig. 5.** The apparent values of  $N$  and  $\Delta H$  mainly differ from their real values (1.0 and  $-1000$ ) for samples of weakly binding **H** with broad distributions. Results are for titrations of 10 mM **H** into 1 mM **M**.

titrations of **M** into **H**, with the notable difference that  $N'$  becomes too small and the numerical value of  $\Delta H'$  increases (Figs. S4 and S5).

### 3.4. Consequences of heterogeneity in $K$ , constant $\Delta H$

In summary, ITC experiments with a heterogeneous binding partner results in normal enthalpograms that can be fitted by the standard single-site model. Thus, heterogeneous binding is not readily detected in a standard ITC binding experiment. The obtained binding constant, however, is only an apparent binding constant and may be somewhat smaller than the average of the heterogeneous sample, but never larger. The obtained binding free energy,  $\Delta G^{\circ}$ , is in most cases a good estimate of the real sample average. Likewise, the additional two fit parameters,  $N$  and  $\Delta H$ , are also quite close to their real values, except for enthalpograms without inflection points. Titrations may be performed with the heterogeneous partner in the syringe or in the cell with the former resulting in slightly better estimates of the real binding parameters. Best estimates are obtained for moderate values of the Wiseman  $c$ -value. High values may lead to a significant underestimation of the binding affinity while low values of the Wiseman  $c$ -value leads to errors on  $N$  and  $\Delta H$ .

### 3.5. Heterogeneity in both $K$ and $\Delta H$

In addition to differences in  $K$ , the individual species in  $H$  may have different heats of binding. Due to enthalpy-entropy compensation the binding enthalpy,  $\Delta H$ , is expected to possess a much larger degree of heterogeneity than the binding free energy,  $\Delta G^\circ$ . As shown below,  $\Delta H$  heterogeneity has a much larger impact on the shape of the enthalpograms than the  $\Delta G^\circ$  heterogeneity explored in the previous section. However, if no  $\Delta G^\circ$  heterogeneity is present the impact of  $\Delta H$  heterogeneity reduces to the trivial case where the system is perfectly described by the single-site model with a binding enthalpy equal to the mean value of  $\Delta H$ . To be observable, heterogeneity in  $\Delta H$  must be accompanied by heterogeneity in  $\Delta G^\circ$ .

This section explores the impact on the enthalpograms when  $H$  is heterogeneous in both  $\Delta G^\circ$  and  $\Delta H$ . The binding heats of the individual species are assumed to be linearly related to their individual  $\Delta G^\circ$ , thus, the species of  $H$  are normally distributed with respect to both  $\Delta H$  and  $\Delta G^\circ$ .  $\Delta H$  may be positively or negatively correlated with  $\Delta G^\circ$ . A positive correlation is often observed experimentally, e.g. for natural cyclodextrins [18], modified cyclodextrins [11], and in protein-ligand binding [19,20]. In principle,  $\Delta H$  may also decrease with increasing  $\Delta G^\circ$ . In the following, the standard deviation on  $\Delta H$ ,  $\sigma_{\Delta H}$ , is defined as positive for positive correlation between  $\Delta H$  and  $\Delta G^\circ$  and negative for negative correlation.

The important heterogeneity parameter determining the shape of ITC enthalpograms is not the absolute value of  $\sigma_{\Delta H}$  but instead the relative standard deviation,  $\sigma_{\Delta H}/\mu_{\Delta H}$ . This ratio will for convenience be referred to as  $\gamma$ .

As shown in the Supplementary data the relative contribution of  $\Delta H$  heterogeneity to the enthalpogram is additive and scales with  $\gamma$ :

$$q = q_G + \gamma \Delta q_H^* \quad (9)$$

$q_G$  corresponds to an enthalpogram without  $\Delta H$  heterogeneity, like the ones explored in the previous section. The total heat signal,  $q$ , resulting from heterogeneity in both  $\Delta G^\circ$  and  $\Delta H$  is then found by adding the contribution from  $\Delta H$  heterogeneity to  $q_G$ . The contribution termed  $\Delta q_H^*$  is shown in Fig. 6. The shape and magnitude of this contribution depends on  $\mu_K$  and  $\sigma_K$  but, importantly, not on  $\mu_{\Delta H}$ . It is thus clear that the contribution from  $\Delta H$  heterogeneity increasingly tends to dominate the enthalpograms with increasing values of  $\gamma$ .

In the previous section it was noted that  $\Delta G^\circ$  heterogeneity in itself only led to slight distortions of the enthalpograms. Adding the contribution from  $\Delta H$  heterogeneity (Fig. 6), which strongly deviates from the

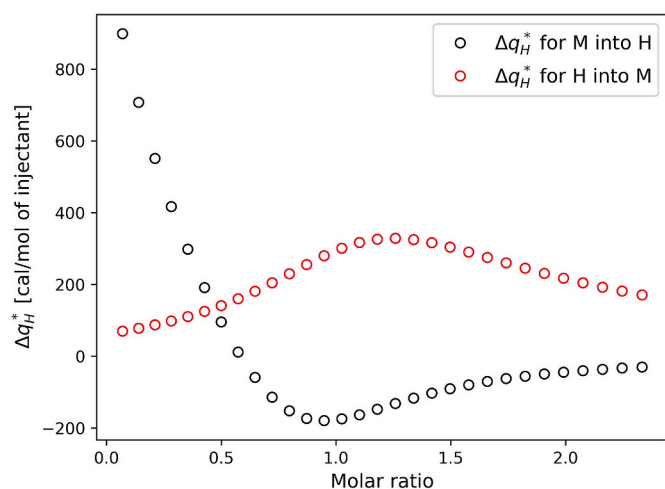


**Fig. 6.** The contribution from  $\Delta H$  heterogeneity, expressed as  $\Delta q_H^*$ , generally has a larger impact when  $H$  is in the cell. Simulation parameters were:  $\mu_K = 50 \times 10^3 \text{ M}^{-1}$ ,  $\sigma_K = 100 \times 10^3 \text{ M}^{-1}$ ,  $\sigma_{\Delta H} = -1000 \text{ cal/mol}$  (i.e.  $\gamma = 1$  when  $\mu_{\Delta H} = -1000 \text{ cal/mol}$ ).

single-site model, will cause serious distortions of the resulting enthalpograms, depending on the sign and magnitude of  $\gamma$ . Such impacts are illustrated by the enthalpograms in Fig. 7 which were generated with the same parameters as in Fig. 3, except that  $\Delta H$  heterogeneity was introduced by setting  $\gamma$  to  $\pm 0.5$ . Thus, the enthalpograms with  $\gamma = 0$  in Fig. 7 correspond to  $q_G$ . Addition or subtraction of  $0.5 \times \Delta q_H^*$  results in the enthalpograms with  $\gamma$  set to  $\pm 0.5$ , i.e.  $\sigma_{\Delta H} = \pm 500 \text{ cal/mol}$ .

The situation for the titration of  $H$  into  $M$  (Fig. 7A) is first discussed. When  $\gamma = 0.5$  the most striking effect is the presence of positive heat signals after the equimolar ratio. The reaction apparently changes from exo- to endothermic! The few percent of slightly endothermic binders present in the distribution are not the cause of the endothermic signal. Instead, the crossover to endothermicity is caused by the displacement of weak binders by strong binders that really sets in after the equimolar ratio (see Fig. 3B). The weakly binding complexes have a more negative binding enthalpy than the strongly binding complexes, resulting in an overall positive heat signal when a strongly binding  $H$  steals an  $M$  from a weakly binding  $H$ .

The opposite situation is observed when the strongly binding  $H$ 's are the most exothermic, that is, when  $\sigma_{\Delta H}$  changes sign and  $\gamma$  becomes negative. Subtraction of  $0.5 \times \Delta q_H^*$  now results in increasingly exothermic signals, particularly around and after the equimolar ratio, due to the increased competition for  $M$ . These distortions of the enthalpograms

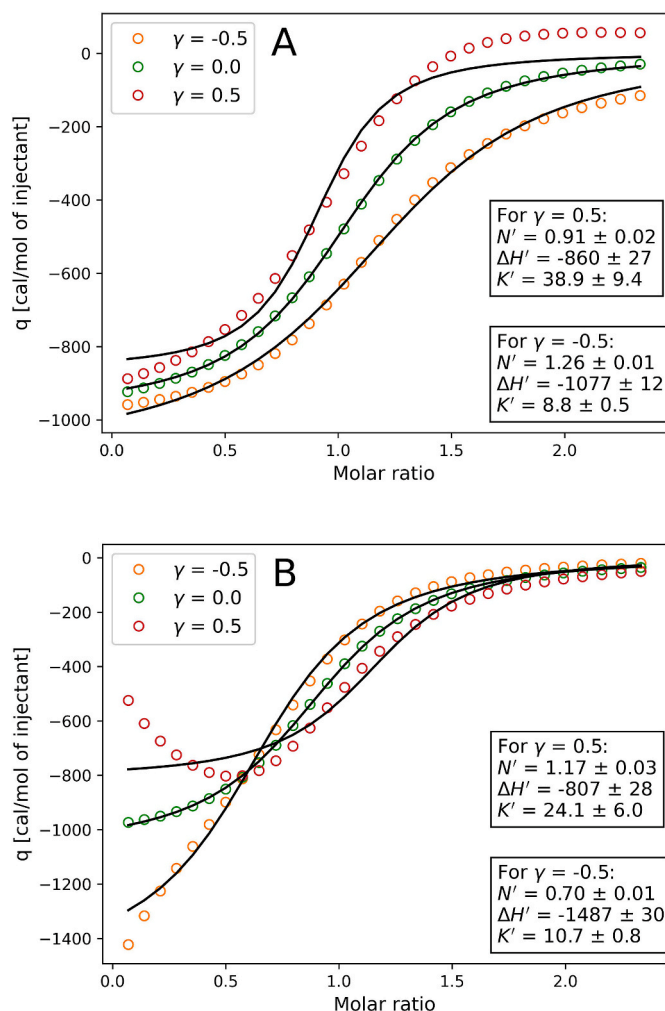


**Fig. 7.** Enthalpograms simulated with the same parameters as in Fig. 3, apart from the introduction of heterogeneity in  $\Delta H$  ( $\gamma \neq 0$ ). Fits of the single-site model to the simulated data are shown as lines. A)  $H$  is titrated into  $M$ . B)  $M$  is titrated into  $H$ .  $K'$  and  $\Delta H'$  are in units of  $10^3 \text{ M}^{-1}$  and  $\text{cal/mol}$ . Simulation parameters were:  $\mu_K = 50 \times 10^3 \text{ M}^{-1}$ ,  $\sigma_K = 100 \times 10^3 \text{ M}^{-1}$ .

affects the fitting parameters, as seen by comparing Fig. 7A to Fig. 3A. Adding the contribution from  $\Delta H$  heterogeneity (positive  $\gamma$ ) causes the fitting function to adopt a steeper shape to capture the heat signals at the end of the titration, i.e. an increase in  $K'$ . Subtraction of the contribution results in a flatter shape of the fitting function, i.e. decreased  $K'$ .

When **M** is titrated into **H** the impact of  $\Delta H$  heterogeneity becomes even more pronounced, as seen in Fig. 7B. The strongest effects are now observed at the beginning of the titration where competition for the small amount of injected **M** is the strongest (see Fig. 3D). Initially, the strongest binders dominate the heat signal, whereas the contribution from the weak binders gradually increases as the strong **H**'s become saturated. When  $\gamma$  is positive, the strong binders are the least exothermic and this results in a minimum in the enthalpogram. The single-site model can only produce monotonously decreasing heat signals and therefore gives a very poor fit. When  $\gamma$  is negative, the enthalpogram does not exhibit a local extremum and a better fit is obtained.

It is clear that introduction of  $\Delta H$  heterogeneity impacts much more on the enthalpograms compared to heterogeneity on only  $K$ . As exemplified on Fig. 7  $\Delta H$  heterogeneity may result in enthalpograms that are poorly described by the single-site model. This may cause researchers to interpret the data in terms of other and more complex binding models. Such misinterpretations are especially likely for positive values of  $\gamma$  where enthalpograms may exhibit a thermal crossover (Fig. 7A) or local extremum (Fig. 7B). For negative values of  $\gamma$  reasonable fits are mostly obtained but the parameters may be strongly misleading. In the case of small  $\mu_{\Delta H}$  the contribution from  $\Delta H$  heterogeneity will dominate, leading to enthalpograms resembling Fig. 6. The Supplementary data contains a further analysis and discussion of the impact of  $\Delta H$  heterogeneity on the quality of the fits and the impact on apparent binding parameters.

### 3.6. Observed heterogeneity in experimental ITC studies

The present investigation was partly motivated by numerous ITC experiments involving modified cyclodextrins binding to small guest molecules [6,11,21]. Despite the heterogeneous character of the cyclodextrins these systems seemed almost exemplary when studied by ITC. The single-site model provided excellent fits to most experiments, stoichiometries were close to 1, and the temperature variation of the binding constant depended on the obtained binding enthalpies as predicted by the van't Hoff equation. Heterogeneity seemed unimportant. However, small problems were occasionally encountered in the form of deviating stoichiometries [10] that varied with temperature [22], systematic variations in the residuals from the fits, and in some cases enthalpograms that strongly deviated from the single-site model. Is it possible that these anomalies can be explained by the heterogeneity of the cyclodextrin samples? Fig. 8 shows the fitted enthalpograms from the titration of 1-adamantaneacetic acid (Ad) with a hydroxypropylated  $\beta$ -cyclodextrin (HPCD) and the reverse titration (Ad into HPCD). Good fits are obtained with the single-site model but the binding parameters differ a lot. The stoichiometry is too high and too low, respectively, and the binding enthalpy differs by a factor of 2! If only the first titration had been conducted one would not suspect a problem, only the additional experiment indicates that something is wrong.

The large discrepancies between the apparent binding parameters from the normal and reverse titration can be explained in qualitative terms by drawing on the theoretical results from the previous sections. First, it is noted that experiments show a strong positive correlation between  $\Delta H$  and  $\Delta G$  for this type of system [11], i.e.  $\sigma_{\Delta H}$  is positive. Together with the exothermicity of the binding reaction, i.e. negative  $\mu_{\Delta H}$ , the titrations in Fig. 8 are in the regime of negative  $\gamma$ . In this regime, Figs. S6 and S7 predict that the titration of HPCD into Ad should yield an overestimated value of  $N$ , and the reverse titration a highly underestimated value of  $N$ . The normal titrations should yield a  $\Delta H'$  close to  $\mu_{\Delta H}$  while the reverse titrations should produce a more negative value. This is exactly what is observed in Fig. 8.

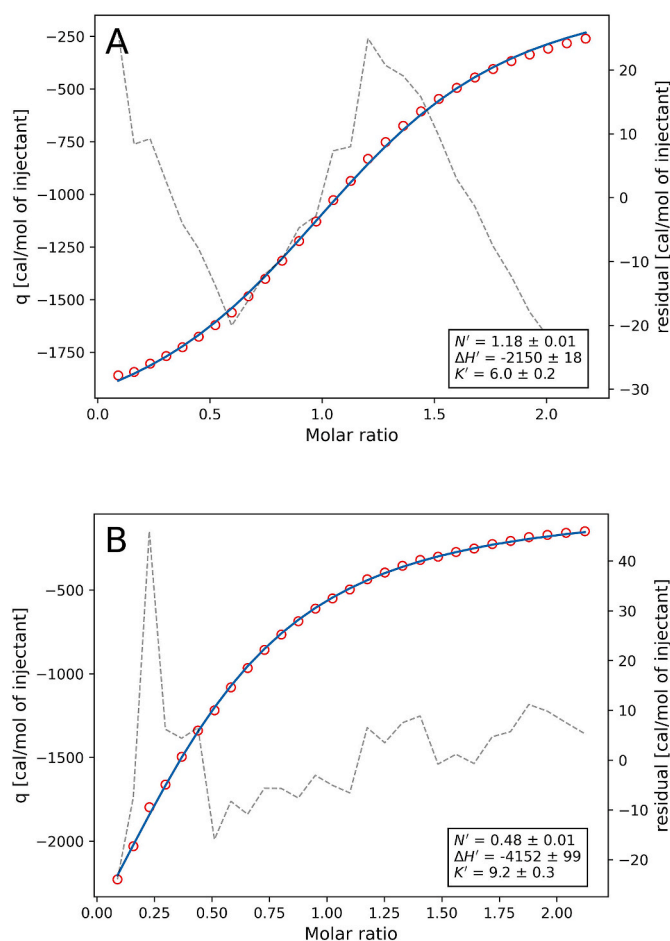


**Fig. 8.** Titrations of 1-adamantaneacetic acid with a hydroxypropylated  $\beta$ -cyclodextrin (A) and the reverse titration (B), both conducted at 25 °C.  $K$  and  $\Delta H$  are in units of  $10^3 \text{ M}^{-1}$  and cal/mol. Experimental details are described in reference 11.

Variation of the experimental temperature provides further evidence of heterogeneity. Binding enthalpies generally depend on temperature, and for cyclodextrin complexes the temperature dependence of  $\Delta H$  is typically in the order of  $-100 \text{ cal/mol}$  for each degree Celsius [7, 22–24]. Thus, the value of  $\gamma$  can be systematically varied by changing the temperature. The temperature dependence of  $\Delta H$  sometimes results in reaction heats that are exactly zero, occurring at the temperature where the reaction crosses from endothermic to exothermic. In the following, this temperature is referred to as the athermal temperature. Linear extrapolation of binding enthalpies from the titrations of HPCD into Ad in the interval 25–55 °C (Fig. S9) reveals an athermal temperature around 10 °C. That is,  $\mu_{\Delta H}$  is expected to be close to 0 around this temperature.  $\Delta H$  heterogeneity is thus expected to have the largest impact near this temperature where the value of  $\gamma$  approaches infinity. Conversely, increasing the temperature away from 10 °C should reduce the impact of  $\Delta H$  heterogeneity. This is exactly what is observed for the titrations in the interval 10–55 °C (Fig. S9). The fits of the single-site model to the titrations at 10 °C are extremely poor and yields unrealistic and inconsistent binding parameters. As the temperature is increased, the fits gradually improve and parameters from the normal and reverse titrations become more realistic and consistent.

These observations are not unique for this system. Titrations of other guest molecules with various modified cyclodextrins all gave rise to odd-shaped enthalpograms at the athermal temperature and deviating stoichiometries in the vicinity of the athermal temperature (data not shown).

### 3.7. Assessment of $\sigma_K$ and $\sigma_{\Delta H}$ in experimental systems with modified cyclodextrins

As discussed above, there are strong indications that ITC titrations with HPCD exhibit  $\Delta H$  heterogeneity. From previous structural and thermodynamic studies it is possible to assess the degree of  $\Delta H$  heterogeneity, as quantified by  $\sigma_{\Delta H}$ . This may be compared to values of  $\sigma_{\Delta H}$  obtained from fitting the heterogeneous model to the abnormal enthalpograms close to the athermal temperature.

An analysis of previously published thermodynamic data for the binding of Ad to various samples of HPCD provides an estimate of the degree of heterogeneity in  $\Delta H$  and  $\Delta G$  for this particular system (analysis is provided in the [Supplementary data](#)). The analysis suggests a  $\sigma_{\Delta H}$  on the order of 3.1 kJ/mol for the binding of HPCD to Ad at 25 °C and a  $\sigma_{\Delta G}$  of around 1.4 kJ/mol, equivalent to  $\sigma_K/\mu_K$  around 0.6 according to equation (2). These values should be considered a lower estimate of the sample heterogeneity as not all aspects of the structural heterogeneity were considered in the analysis.

More accurate estimates of binding heterogeneity may, in principle, be obtained directly from the ITC data by fitting the heterogeneity model to a single enthalpogram that displays clear signs of  $\Delta H$  heterogeneity. This model has 5 parameters:  $\mu_K$ ,  $\sigma_K$ ,  $\mu_{\Delta H}$ ,  $\sigma_{\Delta H}$ , and  $N$ . Keeping the latter fixed at a value of 1.0 results in good fits to the normal and reverse titrations at 10 °C where the effects of  $\Delta H$  heterogeneity are pronounced ([Fig. 9](#)). Judging from the standard deviation on the fit parameters it seems that  $\mu_K$ ,  $\sigma_K$ ,  $\mu_{\Delta H}$  and  $\sigma_{\Delta H}$  are all determined rather

precisely but this is misleading. Unfortunately, it turns out that these parameters depend strongly on the value of  $N$ . Letting  $N$  float results in standard errors of the same magnitude as the parameters themselves. It is also noted that very different values of  $\mu_K$  and  $\sigma_K$  are obtained from the two titrations. On the other hand, the values of  $\mu_{\Delta H}$  and  $\sigma_{\Delta H}$  are quite consistent.  $\mu_{\Delta H}$  is in both cases very close to 0, in agreement with what was concluded by extrapolation of binding enthalpies at higher temperatures.  $\sigma_{\Delta H}$  at 10 °C is around 4–5 kJ/mol, not much larger than the lower estimate of 3.1 kJ/mol that was estimated from thermodynamic data at 25 °C. Also the value of  $\sigma_K/\mu_K$  is more than twice as large as the lower estimate of 0.6.

At higher temperatures it proved more difficult to obtain precise estimates of the heterogeneity parameters from the fits of heterogeneous model to enthalpograms. This is not surprising as these data were well described by the single-site model, and the introduction of additional fitting parameters leads to over-parameterization of the model. Only the reverse titration at 25 °C with the strongly deviating values of  $N$  yielded relative precise parameters when fitted with the heterogeneous model with  $N$  fixed at 1.0 ([Fig. S10](#)).

To summarize, heterogeneity in  $K$  and  $\Delta H$  can quantitatively explain the strange looking enthalpograms at 10 °C and qualitatively explain the anomalies observed at higher temperatures. Reasonable estimates of the heterogeneity parameters can be obtained by fitting the heterogeneous model to titrations near the athermal temperature.

## 4. Discussion

When considering binding heterogeneity the first question is probably: How reliable are the binding parameters that are obtained when fitting the single-site model to experimental data from heterogeneous systems? It is intuitive to assume that the obtained binding constant and binding enthalpy will be a population-weighted average of the species in the heterogeneous system [10,25]. The present investigation shows that this assumption is valid in many cases, at least when the single-site model gives a good fit to enthalpograms that possess an inflection point (i.e. a sufficiently large Wiseman  $c$ -value). The obtained  $K$  may be somewhat lower than the sample average but the apparent free energy of binding is a good estimate of the sample average. Best results are obtained when the heterogeneous component is in the syringe.

Significant problems arise when  $\Delta H$  heterogeneity really sets in but these should be obvious as the enthalpograms tend to deviate significantly from the shape of the single-site model. A more likely pitfall is that the data may be fitted with more complex, but wrong, binding models. It is tempting to interpret enthalpograms with extrema and/or thermal crossovers ([Figs. 7 and 9](#)) in terms of a two-site binding model. Prevette et al. for example, employ a two-site model to analyze ITC titrations of a homogeneous dendrimer into heterogeneous samples of glycosaminoglycans [26]. It is not unreasonable to think that the complex thermograms in [Fig. 4](#) of the article by Prevette et al. is a reflection of sample heterogeneity rather than the proposed aggregation of complexes that is thought to constitute the second binding event. Miskolczy et al. conducted ITC titrations of berberine into heterogeneous sulfo-butylated  $\beta$ -cyclodextrin and obtained an enthalpogram with a local minimum ([Fig. 5](#) in Miskolczy et al.) [27]. This was interpreted as a consecutive formation of 2:1 complexes but could instead be a heterogeneity effect. ITC studies of protein-surfactant interactions also resulted in rather complex enthalpograms, where local extrema and inflection points were thought to indicate transitions [28]. It is thought-provoking that heterogeneity of simple 1-to-1 binding systems, as investigated in the present work, may also produce local extrema.

So how can binding heterogeneity be detected? One may exploit the effects of  $\Delta H$  heterogeneity that become obvious at large values of  $\gamma$ , that is, in the vicinity of the athermal point. Heterogeneity may thus be detected in systems that exhibit apparent single-site behavior by varying the temperature to see whether the single-site model breaks down near the athermal temperature. Conversely, heterogeneity-induced

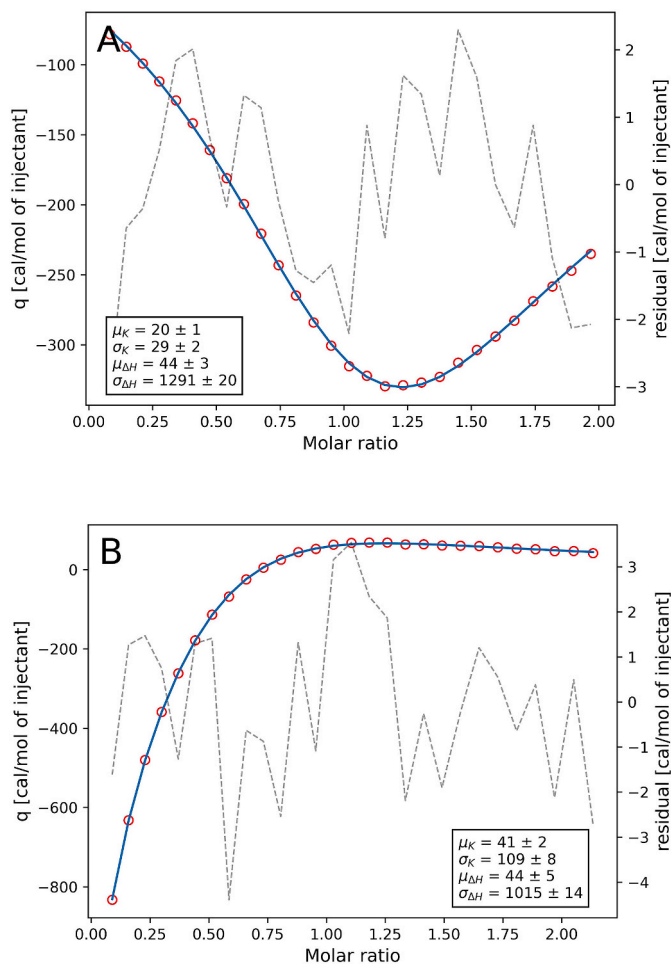


**Fig. 9.** Fits of the heterogeneous model to experimental data from titrations of A) HPCD into Ad and B) Ad into HPCD at 10 °C. The parameter  $N$  is fixed at a value of 1.0.  $K$  and  $\Delta H$  are in units of  $10^3 \text{ M}^{-1}$  and cal/mol.

complexity of the enthalpograms will disappear if the temperature is shifted away from the athermal point. ITC experiments at a range of temperatures are always valuable as it allows for validation of the binding parameters via the van't Hoff equation. Unphysical parameters resulting from application of the wrong binding model will result in deviations from the van't Hoff equation [29,30].

## 5. Conclusion

The almost perfect fits of the standard single-site model to ITC titrations involving a heterogeneous component means that binding heterogeneity in many cases may go unnoticed while still affecting the obtained binding parameters. The apparent binding constant may be significantly lower than the sample average but the obtained binding free energy is a decent estimate of the sample average. Heterogeneity may induce small deviations on the stoichiometry  $N$ , and the binding enthalpy will deviate from the sample average, most significantly when the homogenous component,  $M$ , is titrated into the heterogeneous component,  $H$ , why it is recommended to have  $H$  in the syringe.

Heterogeneity effects dramatically increase when the spread in binding enthalpy is comparable or larger than the average binding enthalpy of the heterogeneous system. For titrations of  $H$  into  $M$ , heterogeneity mainly affects the last part of the enthalpograms while the initial part is affected for titrations of  $M$  into  $H$ .  $\Delta H$  heterogeneity may cause strong distortions of the enthalpograms, including local extrema and thermal crossovers, which can easily be misinterpreted as deriving from multi-site binding or other complex binding models.

When using the single-site model to fit ITC data from heterogeneous systems the obtained binding parameters most correctly represent the sample average when 1) concentrations are chosen to produce soft S-shaped enthalpograms 2) the heterogeneous component is in the syringe 3) titrations are conducted at a temperature where  $\gamma$  is small and negative.

## CRedit authorship contribution statement

**Christian Schönbeck:** Conceptualization, Data curation, Formal analysis, Investigation, Methodology, Software, Validation, Visualization, Writing – original draft, Writing – review & editing. **Jeppe Kari:** Conceptualization, Methodology, Writing – original draft. **Peter Westh:** Funding acquisition, Resources, Supervision, Writing – original draft.

## Declaration of competing interest

The authors declare that they have no known competing financial interests or personal relationships that could have appeared to influence the work reported in this paper.

## Data availability

Python code and experimental data are available via the link to Google Colab in the article.

## Appendix A. Supplementary data

Supplementary data to this article can be found online at <https://doi.org/10.1016/j.ab.2023.115446>.

## References

- [1] H.J. An, J.W. Froehlich, C.B. Lebrilla, Determination of glycosylation sites and site-specific heterogeneity in glycoproteins, *Curr. Opin. Biol. Sci.* 13 (2009) 421–426, <https://doi.org/10.1016/j.cbpa.2009.07.022>.
- [2] J.X. Huang, M.A. Cooper, M.A. Baker, M.A.K. Azad, R.L. Nation, J. Li, T. Velkov, Drug-binding energetics of human  $\alpha$ -1-acid glycoprotein assessed by isothermal titration calorimetry and molecular docking simulations, *J. Mol. Recogn.* 25 (2012) 642–656, <https://doi.org/10.1002/jmr.2221>.
- [3] F. Zsila, T. Juhász, G. Kohut, T. Beke-Somfai, Heparin and heparan sulfate binding of the antiparasitic drug imidocarb: circular dichroism spectroscopy, isothermal titration calorimetry, and computational studies, *J. Phys. Chem. B* 122 (2018) 1781–1791, <https://doi.org/10.1021/acs.jpcc.7b08876>.
- [4] R. Garcia-Valls, T.A. Hatton, Metal ion complexation with lignin derivatives, *Chem. Eng. J.* 94 (2003) 99–105, [https://doi.org/10.1016/S1385-8947\(03\)00007-X](https://doi.org/10.1016/S1385-8947(03)00007-X).
- [5] A. Hawe, T. Rispen, J.N. Herron, W. Jiskoot, Probing bis-ANS binding sites of different affinity on aggregated IgG by steady-state fluorescence, time-resolved fluorescence and isothermal titration calorimetry, *J. Pharm. Sci.* 100 (2011) 1294–1305, <https://doi.org/10.1002/jps.22368>.
- [6] C. Schönbeck, P. Westh, J.C. Madsen, K.L. Larsen, L.W. Ståde, R. Holm, Methylated  $\beta$ -cyclodextrins: influence of degree and pattern of substitution on the thermodynamics of complexation with tauro- and glyco-conjugated bile salts, *Langmuir* 27 (2011) 5832–5841, <https://doi.org/10.1021/la200381f>.
- [7] E. Berta, D. Landy, Improving ITC studies of cyclodextrin inclusion compounds by global analysis of conventional and non-conventional experiments, *Beilstein J. Org. Chem.* 10 (2014) 2630–2641, <https://doi.org/10.3762/bjoc.10.275>.
- [8] Y. Zheng, L.N. Dong, M. Liu, A. Chen, S. Feng, B. Wang, D. Sun, Effect of pH on the complexation of kaempferol-4'-glucoside with three  $\beta$ -cyclodextrin derivatives: isothermal titration calorimetry and spectroscopy study, *J. Agric. Food Chem.* 62 (2014) 244–250, <https://doi.org/10.1021/jf404320w>.
- [9] G.L. Perlovich, M. Skar, A. Bauer-Brandl, Driving forces and the influence of the buffer composition on the complexation reaction between ibuprofen and HPCD, *Eur. J. Pharmaceut. Sci.* 20 (2003) 197–200, [https://doi.org/10.1016/S0928-0987\(03\)00180-5](https://doi.org/10.1016/S0928-0987(03)00180-5).
- [10] C. Schönbeck, P. Westh, J.C. Madsen, K.L. Larsen, L.W. Ståde, R. Holm, Hydroxypropyl-substituted  $\beta$ -cyclodextrins: influence of degree of substitution on the thermodynamics of complexation with tauroconjugated and glycoconjugated bile salts, *Langmuir* 26 (2010) 17949–17957, <https://doi.org/10.1021/la103124n>.
- [11] C. Schönbeck, R. Holm, Exploring the origins of enthalpy–entropy compensation by calorimetric studies of cyclodextrin complexes, *J. Phys. Chem. B* 123 (2019) 6686–6693, <https://doi.org/10.1021/acs.jpcc.9b03393>.
- [12] T. Wiseman, S. Williston, J.F. Brandts, L.N. Lin, Rapid measurement of binding constants and heats of binding using a new titration calorimeter, *Anal. Biochem.* 179 (1989) 131–137, [https://doi.org/10.1016/0003-2697\(89\)90213-3](https://doi.org/10.1016/0003-2697(89)90213-3).
- [13] L.D. Hansen, G.W. Fellingham, D.J. Russell, Simultaneous determination of equilibrium constants and enthalpy changes by titration calorimetry: methods, instruments, and uncertainties, *Anal. Biochem.* 409 (2011) 220–229, <https://doi.org/10.1016/j.ab.2010.11.002>.
- [14] V. Paketytytė, V. Petrauskas, A. Zubrienė, O. Abian, M. Bastos, W.Y. Chen, M. J. Moreno, G. Krainer, V. Linkuvienė, A. Sedivy, A. Velazquez-Campoy, M. A. Williams, D. Matulis, Uncertainty in protein–ligand binding constants: asymmetric confidence intervals versus standard errors, *Eur. Biophys. J.* 50 (2021) 661–670, <https://doi.org/10.1007/s00249-021-01518-4>.
- [15] Marco Taboga, “Log-normal Distribution”, Lectures on Probability Theory and Mathematical Statistics, 2021. <https://www.statlect.com/Probability-Distributions/Log-Normal-Distribution>.
- [16] MicroCal, *ITC Data Analysis in Origin*, 2004.
- [17] A. Velazquez-Campoy, B. Claro, O. Abian, J. Höring, L. Bournon, R. Claveria-Gimeno, E. Ennifar, P. England, J.B. Chaires, D. Wu, G. Piszczek, C. Brautigam, S. C. Tso, H. Zhao, P. Schuck, S. Keller, M. Bastos, A multi-laboratory benchmark study of isothermal titration calorimetry (ITC) using Ca<sup>2+</sup> and Mg<sup>2+</sup> binding to EDTA, *Eur. Biophys. J.* 50 (2021) 429–451, <https://doi.org/10.1007/s00249-021-01523-7>.
- [18] M.v. Rekharsky, Y. Inoue, Complexation thermodynamics of cyclodextrins, *Chem. Rev.* 98 (1998) 1875–1918, <https://doi.org/10.1021/cr970015o>.
- [19] J. Mecnović, P.W. Snyder, K.A. Mirica, S. Bai, E.T. MacK, R.L. Kwant, D. T. Moustakas, A. Héroux, G.M. Whitesides, Fluoroalkyl and alkyl chains have similar hydrophobicities in binding to the “hydrophobic wall” of carbonic anhydrase, *J. Am. Chem. Soc.* 133 (2011) 14017–14026, <https://doi.org/10.1021/ja2045293>.
- [20] P.W. Snyder, J. Mecnović, D.T. Moustakas, S.W. Thomas, M. Harder, E.T. Mack, M. R. Lockett, A. Héroux, W. Sherman, G.M. Whitesides, Mechanism of the hydrophobic effect in the biomolecular recognition of arylsulfonamides by carbonic anhydrase, *Proc. Natl. Acad. Sci. U. S. A.* 108 (2011) 17889, <https://doi.org/10.1073/pnas.1114107108>. –17894.
- [21] C. Schönbeck, P. Westh, R. Holm, Complexation thermodynamics of modified cyclodextrins: extended cavities and distorted structures, *J. Phys. Chem. B* 118 (2014) 10120–10129, <https://doi.org/10.1021/jp506001j>.
- [22] C. Schönbeck, R. Holm, P. Westh, G.H. Peters, Extending the hydrophobic cavity of  $\beta$ -cyclodextrin results in more negative heat capacity changes but reduced binding affinities, *J. Inclusion Phenom. Macrocycl. Chem.* 78 (2014) 351–361, <https://doi.org/10.1007/s10847-013-0305-2>.
- [23] P.D. Ross, M.V. Rekharsky, Thermodynamics of hydrogen bond and hydrophobic interactions in cyclodextrin complexes, *Biophys. J.* 71 (1996) 2144–2154, [https://doi.org/10.1016/S0006-3495\(96\)79415-8](https://doi.org/10.1016/S0006-3495(96)79415-8).
- [24] C. Schönbeck, T.L. Madsen, G.H. Peters, R. Holm, T. Loftsson, Soluble 1:1 complexes and insoluble 3:2 complexes – understanding the phase-solubility diagram of hydrocortisone and  $\gamma$ -cyclodextrin, *Int. J. Pharm.* 531 (2017) 504–511, <https://doi.org/10.1016/j.ijpharm.2017.05.024>.
- [25] A.K. Dutta, J. Rösger, K. Rajarathnam, Using isothermal titration calorimetry to determine thermodynamic parameters of protein–glycosaminoglycan interactions, in: *Methods in Molecular Biology*, Humana Press Inc., 2015, pp. 315–324, [https://doi.org/10.1007/978-1-4939-1714-3\\_25](https://doi.org/10.1007/978-1-4939-1714-3_25).
- [26] L.E. Prevette, N.C. Benish, A.R. Schoenecker, K.J. Braden, Cell-penetrating compounds preferentially bind glycosaminoglycans over plasma membrane lipids

- in a charge density- and stereochemistry-dependent manner, *Biophys. Chem.* 207 (2015) 40–50, <https://doi.org/10.1016/j.bpc.2015.08.003>.
- [27] Z. Miskolczy, M. Megyesi, L. Biczók, Entropy-driven inclusion of natural protoberberine alkaloids in sulfobutylether- $\beta$ -cyclodextrin, *Molecules* 27 (2022) 7514, <https://doi.org/10.3390/molecules27217514>.
- [28] F.G. Tidemand, A. Zunino, N.T. Johansen, A.F. Hansen, P. Westh, K. Mosegaard, L. Arleth, Semi-empirical analysis of complex ITC data from protein–surfactant interactions, *Anal. Chem.* (2021), <https://doi.org/10.1021/acs.analchem.1c02558>.
- [29] C. Schönbeck, R. Holm, P. Westh, Higher order inclusion complexes and secondary interactions studied by global analysis of calorimetric titrations, *Anal. Chem.* 84 (2012) 2305–2312, <https://doi.org/10.1021/ac202842s>.
- [30] S.A. Kantonen, N.M. Henriksen, M.K. Gilson, Accounting for apparent deviations between calorimetric and van't Hoff enthalpies, *Biochim. Biophys. Acta Gen. Subj.* 1862 (2018) 692–704, <https://doi.org/10.1016/j.bbagen.2017.11.020>.